2022 19th International Conference on Electrical Engineering, Computing Science and Automatic Control (CCE). Mexico City, Mexico. November 9-11, 2022

J Wave Detection Algorithm of the BCG in Chair and Bed using Continuous Spline Wavelet Transform

Laura Ivonne Flores-Nuñez
Bioelectronics Section
Electrical Engineering Department, CINVESTAV
Mexico City, Mexico
laura.florezn@cinvestav.mx

José Alberto García-Limón
Bioelectronics Section
Electrical Engineering Department, CINVESTAV
Mexico City, Mexico
josea.garcial@cinvestav.mx

Frank Martínez-Suárez
Bioelectronics Section
Electrical Engineering Department, CINVESTAV
Mexico City, Mexico
frank.martinez@cinvestav.mx

Ramon Casanella
Universitat Politècnica de Catalunya BarcelonaTech, Castelldefels School of Telecommunications and Aerospace Engineering, Spain
ramon.casanella@upc.edu

Carlos Alvarado-Serrano
Bioelectronics Section
Electrical Engineering Department, CINVESTAV
Mexico City, Mexico
calvarad@cinvestav.mx

***Abstract*- This study presents an algorithm for unsupervised beat-to-beat detection of the J-wave of the ballistocardiogram (BCG) in records of both lying (bed) and seated (chair) persons. The algorithm is based on the continuous wavelet transform (CWT) with splines, which offers the advantage of using a wide range of scales and the reduction of noise and mechanical interference. For J-wave detection, the most prominent negative modulus of the CWT is detected using adaptive time windows (the negative modulus provides more information about the location of the J-wave), and then a confirmation is performed from temporal and amplitude parameters. Seven records from a chair database and fifteen records from a bed database were used to evaluate the algorithm. To assess the J-wave detection, the Bland Altman test was used, measuring the heart rate (HR) from the ECG as a reference and considering a 95% confidence interval (±2 SD). For the bed database the mean error was -0.03 beats/min with a confidence interval of ±3.87 and for the chair database the mean error was -0.05 beats/min with a confidence interval of ±3.48 beats/min. Results satisfied the standards for HR meters recommended by the Association for the Advancement of Medical Instrumentation (AAMI).**

Keywords- BCG, Wavelet Transform, Heart Rate.

I. INTRODUCTION

There is a growing demand for monitoring technologies in non-hospital environments (home monitoring) for vital parameters such as heart rate (HR), blood pressure, respiratory rate, etc. This trend is an important step towards the prevention, prediction and treatment of cardiovascular diseases [1]. Advances in sensor technology in terms of cost and size have renewed the interest and prominence of the ballistocardiogram (BCG), different continuous monitoring systems have been proposed by embedding sensors of different types in everyday objects such as office chairs [2], [3], wheelchairs [4], beds [5] and weighing scales [6].

The BCG is a record of the micromovements of the body produced by the recoil forces generated in each heartbeat due to changes in the center of mass by the rapid acceleration of the blood as it is ejected through the vascular tree. These forces can be measured as displacement, velocity, or acceleration in three different geometric axes: head-to-foot (longitudinal or vertical), dorsoventral (transverse or antero-posterior) and lateral (left-right) [7]. Fig. 1 shows the typical BCG with letters identifying each of its parts [8]. The J-wave is the highest amplitude positive wave after the cardiac cycle, which is frequently used as a reference.

A major challenge in the development of algorithms for automatic detection of BCG waves is that the morphology varies between subjects, measurement device and the measurement axis [9]. Therefore, several automatic algorithms for J-wave and thus HR detection have been proposed, most of them focusing on single-position, single-axis BCG recordings, also because few public databases exist.

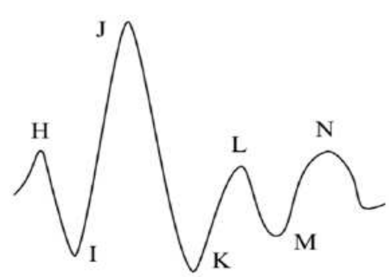

Fig.1. Typical form of the normal ballistocardiogram [8].

This work has been funded by a scholarship from the CONACYT (México) to Laura Ivonne Flores Nuñez

Techniques vary from algorithms based on the signal envelope [10], filters [11], Continuous Wavelet Transform (CWT) [12], [13], Discrete Wavelet Transform (DWT) [14], Multiresolution Analysis of the Maximal Overlap Discrete Wavelet Transform (MODWT-MRA) [15] and adaptive beat shape modeling [16]. Methods based on wavelet analysis have proven to be successful regardless of the type of sensors or experimental setups [17], in addition to being effective for processing nonlinear and non-stationary physiological signals [18], [19].

In this work we propose an algorithm based on CWT with splines for the J-wave detection of the BCG regardless of the type of sensor or the measurement axis. To assess its performance, two databases consisting in 7 records of chair-based BCG [9] and 15 records of bed-based BCG [20] were used. This algorithm is based on a previous algorithm presented in [12] with important improvements in the detection methodology, to obtain the necessary generality for its operation in either BCG database.

II. MATERIALS AND METHODS

A. BCG and ECG Datasets

The first database (Chair) used was acquired by a piezoelectric sensor attached to the bottom side of the seat of a chair, the BCG was measured over the longitudinal axis, the ECG (lead 1) was acquired simultaneously and both signals were digitized at a sampling rate of 1 kHz and band limited between 0.5–20 Hz and 0.16–100 Hz respectively, as referred in [9]. General subjects information is summarized in Table 1.

TABLE I
DATABASE CHARACTERISTICS

Database	Subjects	Sex	Age	Weight [Kg]	Height [m]
Chair	7	5 M & 2 F	33±6	67 to 87	1.65 to 1.75
Bed	15	8 M & 7 F	27±5	48 to 94	1.53 to 1.97

In the second database used (Bed) published in 2020 [20], the BCG was acquired on the transverse axis through a set of 4 EMFi sensors placed centrally on the base of a bed and 4 load cells positioned under the bedposts. The signals obtained from each sensor were visually analyzed determining greater correspondence of the BCG with the EMFi sensor "Film 0". From this database of 40 subjects, 15 subjects were chosen, having similar age, weight, and height ranges to those of the first database. Each of the signals was band limited between 0.3–24 Hz, simultaneously obtaining the ECG (lead 3) band limited between 0.5–40 Hz with the same sampling rate of 1 kHz.

B. Signal preprocessing

The two datasets were analyzed using Matlab® R2021b, and prior to detection BCG databases were digital bandpass filtered with a FIR zero-phase filter between 0.5–25 Hz of 150th order using Hamming window, to reduce artifacts and to ensure that both databases had the same bandwidth. In addition, the bed database was inverted due to the positioning of the sensor with respect to the subjects' bodies.

C. *J-wave detection using CWT with splines*

The processing tool used for the development of the algorithm was the continuous wavelet transform (CWT) [21] which is defined by the equation (1).

$$CWT_x(a,b) = \int_{-\propto}^{\propto} x(t)\psi^*\left(\frac{t-b}{a}\right)dt \qquad (1)$$

The CWT consists of a convolution integral between a signal x(t) and a wavelet function, which contains two parameters: the translation parameter b and the scale parameter a. Its behavior is to act as a bandpass filter, whose cutoff frequencies are related to the scaling factor a, restricted to discrete values over the sequence 2^j (j=1, 2…), which sometimes can limit the analysis. In this work, we use the *B*-splines functions to evaluate the CWT at any integer scale [22], where its representation is equivalent to a polynomial spline function expressed as

$$CWT(x(t),m,k) = \sum_{k\in Z}\left([p]\uparrow_m * u_m^{n_2} * b^{n_1+n_2+1} * c\right)(k) \qquad (2)$$

where $[p]\uparrow_m (k)$ represents the upsampling of the B-spline coefficients of the wavelet function expanded by a factor of m, $u_m^{n_2}$ refers to a cascade of (n_2 – 1) moving sum filters with the order (m-1) and with a k_0 offset ensuring its symmetry, $b^{n_1+n_2+1}$ is the representation of the B-spline convolution of degree (n_1+n_2+1) between the analyzed function and the wavelet function, and $c(k)'s$ are the B-splines coefficients of the analyzed function.

The approach of this algorithm follows the structure reported in [12] with some important improvements. First, a mother wavelet function equivalent to the first derivative of a fourth-order cubic B-spline considering scale 5 (CWT_5) with cutoff frequencies of 46–155 Hz is used, to improve the characteristics of the waveform. Secondly, to achieve the analysis of two different databases, detection focused on finding the lowest negative peak (W_n) instead of the positive (W_p), because it was found to be the most consistent point in the CWT for the J-wave detection (Fig. 2). Finally, adaptive search windows for minimal changes in HR, point correction by performing forward and backward searches, and the addition of new validation points were implemented, to avoid false negative detection and improve J-wave detection.

The overall detection of the J-wave peak (J_p) is only accepted as true if the local minima W_n and the local maxima W_p exceed the adaptive thresholds and have a reasonable duration. The operation of the algorithm is divided into two stages: a recognition stage and decision stage, as described below.

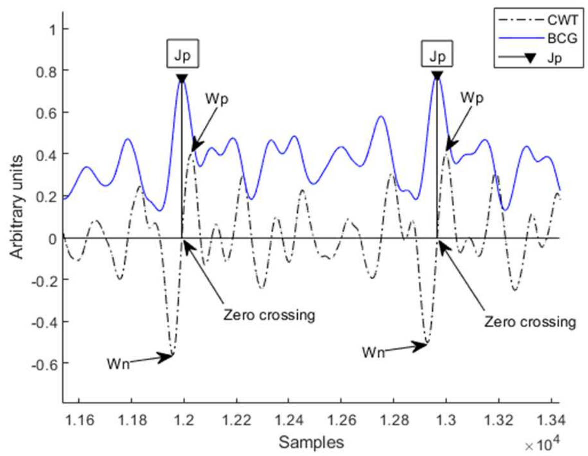

Fig. 2. Comparison of BCG wave and CWT_5 for the J-wave peak detection with Wp, Wn and zero crossing.

1) Recognition stage

This stage as described in [12], defines the first four J waves, corresponding to $J_p(1:4)$. The starting point for the search window corresponds to the refractory period 'Start' which can be variable for each record. Then in the next 2 s the maximum W_p and the minimum W_n are searched establishing the positive threshold $(Pt = V_1 W_P)$ and the negative threshold $(Nt = V_2 W_n)$ where the constants V_1 and V_2 are experimental values corresponding to 0.6 and 0.65 respectively. Once defined, a window search is initiated for the maxima W_p, minima W_n and zero-crossings that are greater than *Pt* and less than *Nt*. Finally, the interval $JJ(1:3)$ and the mean interval JJ_{av} (1:3) are calculated to define the initial search point ($SP = W_{p4} + V_3 * JJ_{av}(1{:}3)$) for the next J_p, with an experimental value of V_3= 0.71.

2) Decision stage

At this stage, we seek to find the next J_p points until the condition that the boundary $\left(LM = SP + V_4 * JJ_{av}(4{:}\mathrm{n})\right)$ exceeds the length of CWT_5, where V_4 was set to 0.75.

For a better understanding of this stage, the procedure will be divided into four steps:

2.1 Search window: once the previous J_p is detected, the search window is limited in order not to detect erroneous points, the initial value is updated with (3) and the final value is determined with (4).

$$SP = W_p + 0.66 * JJ_{av}(n) \qquad (3)$$

$$JJ(n-1) > 1.06 \text{ x } JJ_{av2} \qquad (4)$$

Where $JJ(n-1)$ refers to the previous JJ interval and JJ_{av2} to the average of the two previous intervals $[JJ(\mathrm{n}-2{:}JJ(\mathrm{n}-1)]$.
If the condition (4) is met, then a longer window limit (0.52 x $JJ_{av}(n)$) is considered and if it is not, a normal window limit (0.37 x $JJ_{av}(n)$) is used. With this, an adaptive window is obtained according to the evolution of the subject's HR.

2.2 Detection: To determine the J_p point, first the minimum W_n is detected in the search window, then W_p and the zero crossing between them are searched (Fig. 2). Sometimes when the signals present more than one crossing, the W_p with the highest amplitude is chosen and a short search is made to find the correct point.

2.3 J_p evaluation: The candidate J_{p1} is evaluated under two main criteria: amplitude and time. To make sure that it is within the average respect to the other points, we first calculate the negative interval (CNI) which corresponds to the difference between the W_n and the previous JJ interval $(W_n - J(n-1))$ and then applied the eqs. (5) and (6):

$$CNI > 1.074 * JJ(n-1) \qquad (5)$$

$$\begin{gathered} AW_{n2} < 0.31 * AW_{n1} \\ AW_{p2} > 0.4 * AW_p(n-1) \\ W_{p1} - W_{p2} > SPR \end{gathered} \qquad (6)$$

where the prefix *A* refers to the amplitude of the point analyzed and the SPR factor is variable with a standard value of 240. If (5) is satisfied, a backward search of J_{p1} is performed to find another possible point (J_{p2}). This new point is validated with (6) and if it is true the value of J_{p1} is updated. If this is not fulfilled, J_{p1} is evaluated through the eqs. (7) and (8).

$$\begin{gathered} CNI < 1.07 * JJ(n-1) \\ AW_1 > 0.85 * AW_{nav}(n-3{:}n) \end{gathered} \qquad (7)$$

$$\begin{gathered} CNI_2 < 1.22 * JJ_{av2} \\ A_{BCG}\left(J_{p2}\right) > A_{BCG}\left(J_{p1}\right) \\ AW_{p2} > 0.81 * AW_{p1} \end{gathered} \qquad (8)$$

Where AW_{nav} equals the average of the amplitudes of W_n and A_{BCG} equals the amplitude of the BCG. If (7) and (8) are satisfied a new point J_{p2} beyond the candidate J_{p1} is found and its values are updated, otherwise the value of J_{p1} is retained.

The final evaluation to confirm or reject the J_{p1} position is performed with (9). The experimental value of the minimum negative threshold (umn) was considered as a variable factor with a standard of 0.76, and the maximum threshold (umx) was experimentally set to 1.32. Both factors play a very important role in determining the minimum and maximum percentage of the JJ_{av} as a decisive factor.

$$\begin{gathered} JJ(n) > umn * INJ < umx * INJ \\ AW_p(n) > 0.34 * Pt \end{gathered} \qquad (9)$$

In (9), the interval $JJ(n)$ is obtained from the difference of the J_p found and the previous, and the INJ factor is obtained by averaging the last five JJ intervals (except for the first five, for which the last one is used).

If (9) is false, two more search windows are performed. In the first $(SP-60\text{ ms}: SP+220\text{ ms})$ we search for J_{p3} which is validated with (10). If it is rejected, we perform the last search $(SP+70\text{ ms}: SP+150\text{ ms})$ finding J_{p4} which is verified through (11).

$$JJ(n) > umn * INJ < umx * INJ$$
$$AW_{n3} < 0.55 * Nt \qquad (10)$$

$$JJ(n) > umn * INJ < umx * INJ \qquad (11)$$

2.4 Update: Once the J_p point is confirmed the HR is obtained, the maximum threshold $(Pt = (0.6 * Pt) + (0.4 * Wp))$, the minimum threshold $(Nt = (0.6 * Nt) + (0.4 * Wp))$ and the different JJ_{av}(4:n) used in the algorithm are updated.

The flowchart of the entire algorithm is shown in Fig. 3.

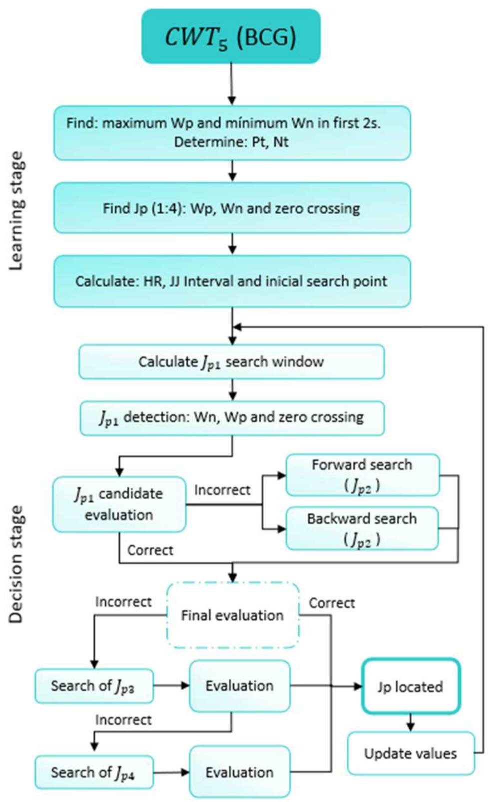

Fig. 3. Flowchart for J-wave detection.

III. RESULTS AND DISCUSSION

To test the algorithm, 22 BCG recordings were used with a duration between 60–100 s for 7 chair recordings and 5–7 min for 15 bed recordings.

The results of the detection performance are presented in tables II and III, where sensitivity (*Se*) and positive predictivity ($P+$) were calculated as a function of the number of *TP* (true positive detections), *FN* (false negative detections) and *FP* (false positive misdetections). In addition, with the aim of quantitatively validating whether the detected points truly corresponded to the J-wave, the Bland-Altman statistical test [23] was carried out in which HR from R-R intervals of the ECG (measured with Alvarado et. al. algorithm [24]) was taken as a reference for the HR obtained from J-J intervals. For the bed database, the results were obtained considering approximately 100 s to match the acquisition time of the chair database.

The algorithm's performance for both databases is shown in the Bland-Altman plots in Fig. 4. And it can be observed that most results fall within the 95% confidence interval (CI) corresponding to ±2 SD. For chair database (Fig. 4a) the CI was ± 3.48 beats/min with a mean error of -0.05 beats/min and for bed database (Fig. 4b), the CI was ±3.87 beats/min with a mean error of -0.03 beats/min (omitting false negatives), demonstrating compliance with the accuracy limits (±5 beats/min) for the HR measurement standard established by the Association for the Advancement of Medical Instrumentation (AAMI) [25].

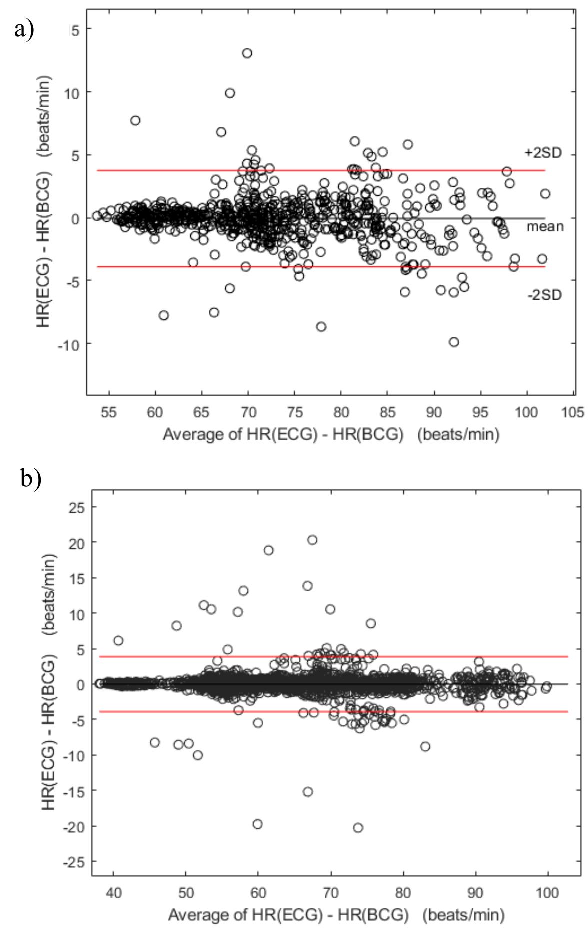

Fig. 4. Bland Altman plots of the average difference of the HR from ECG and the HR from BCG. a) Results for chair database. b) Results of 100 s of bed data base.

A. Results for Jp Detection (Bed)

In this database, 80 *FP* and 8 *FN* were detected out of a total of 6650 beats, having averages of *Se*= 99.89%, *P+*= 98.90% and *TP*=98.79%. As can be noted, one of the advantages of this algorithm is that by using the average of the previously detected points, the probability of early or late detection of a J-wave is reduced. The results for each record analyzed from this database are summarized in Table II.

TABLE II.
J_P DETECTION PERFORMANCE FOR BED DATABASE

BED DATABASE RESULTS						
ID	*TP*	*FP*	*FN*	*Se %*	*P+ %*	*TP%*
X1001	206	2	0	100.00%	99.04%	99.04%
X1004	406	2	0	100.00%	99.51%	99.51%
X1005	536	31	1	99.81%	94.53%	94.37%
X1006	508	0	0	100.00%	100.00%	100.00%
X1007	451	2	0	100.00%	99.56%	99.56%
X1008	356	1	0	100.00%	99.72%	99.72%
X1009	507	12	2	99.61%	97.69%	97.31%
X1022	377	5	1	99.74%	98.69%	98.43%
X1023	367	0	0	100.00%	100.00%	100.00%
X1027	372	5	0	100.00%	98.67%	98.67%
X1031	409	4	1	99.76%	99.03%	98.79%
X1032	529	3	0	100.00%	99.44%	99.44%
X1040	613	6	2	99.67%	99.03%	98.71%
X1044	496	6	1	99.80%	98.79%	98.59%
X1046	435	1	0	100.00%	99.77%	99.77%

B. Results for Jp Detection (Chair)

The number of total beats detected for this database was 779 with 6 *FP* and 0 *FN.* In this case, the achieved averages were *Se*= 100%, *P+*= 99.24% and *TP*=99.24%. In comparison with [12], similar results were obtained with a total of +4 beats. For this database, no false negatives were found because the presence of the J wave in relation to others was evident, something that did not occur in the bed database, since waves with similar characteristics were detected. In addition, the subjects had a more constant HR making their detection more predictable due to the short recordings, compared to the bed database.

TABLE III.
J_P DETECTION PERFORMANCE FOR CHAIR DATABASE

CHAIR DATABASE RESULTS						
ID	*TP*	*FP*	*FN*	*Se %*	*P+ %*	*TP%*
1	108	0	0	100.00%	100.00%	100.00%
2	120	3	0	100.00%	97.56%	97.56%
3	119	0	0	100.00%	100.00%	100.00%
4	137	0	0	100.00%	100.00%	100.00%
5	57	0	0	100.00%	100.00%	100.00%
6	101	3	0	100.00%	97.12%	97.12%
7	131	0	0	100.00%	100.00%	100.00%

In this study, a comparison of amplitude was not possible because the sensors used in the databases were different and therefore, they had a different signal magnitude. Nevertheless, despite the variations in morphology between subjects and the measurement axis, the CTW was able to emphasize J-wave location accurately in most cases. Figure 5 graphically shows its robustness to motion artifacts for a representative chair database record (Fig. 5a), as well as for a bed database record (Fig. 5b), regardless of the differences in the measurement system.

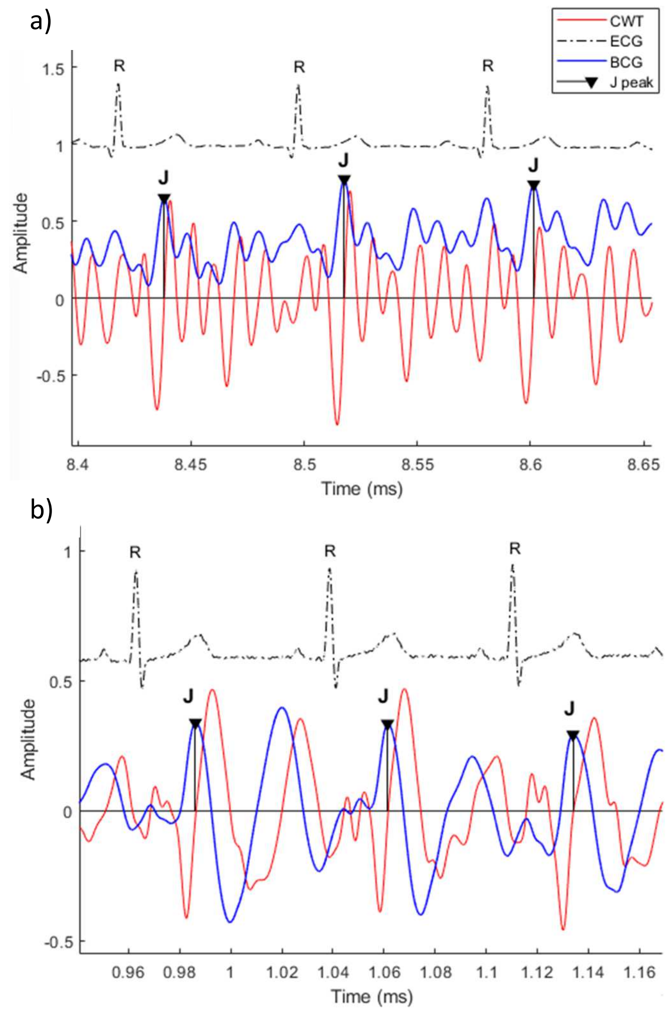

Fig. 5. Segment of a BCG signal with its CWT and ECG. a) Bed database record of subject "X1032". b) Chair database record of subject #7.

IV. CONCLUSION

The detection of BCG waves can be a complex task to perform due to their changing morphology, especially if a reference signal such as the ECG is not being used. To reduce this complexity, we propose the use of continuous wavelet transform with splines, that allow to discard high amplitude and low frequency peaks present in BCG recordings due to baseline variations and mechanical interferences.

The performance of the proposed algorithm was found to be within the accuracy limits established by the AAMI for heart rate measurement, considering that it was calculated from the detection of the J wave in different BCG databases, achieving sufficient generality without focusing on a specific morphology as is generally done.

As future aim, we will continue working on the development of a universal algorithm for automatic unsupervised detection of BCG waves, independent of sensor and measurement axis, to obtain and to analyze more data, to develop BCG technology and to generate medical devices.

REFERENCES

[1] M. A. Konstam, "Home monitoring should be the central element in an effective program of heart failure disease management," *Circulation*, vol. 125, no. 6, pp. 820–827, Feb. 2012, doi: 10.1161/CIRCULATIONAHA.111.031161.

[2] A. R. Malik and J. Boger, "Zero-Effort Ambient Heart Rate Monitoring Using Ballistocardiography Detected Through a Seat Cushion: Prototype Development and Preliminary Study," *JMIR Rehabilitation and Assistive Technologies*, vol. 8, no. 2, Apr. 2021, doi: 10.2196/25996.

[3] P. S. Luna and R. Pallàs, "Automatic Concealed Heart Rate Detection from the BCG in Seated Position," *IEEE Latin America Transactions*, vol. 13, no. 3, pp. 583–588, Mar. 2015, doi: 10.1109/TLA.2015.7069078.

[4] E. Pinheiro, O. Postolache, and P. Girão, "Study on ballistocardiogram acquisition in a moving wheelchair with embedded sensors," *Metrology and Measurement Systems*, vol. 19, no. 4, pp. 739–750, 2012, doi: 10.2478/V10178-012-0065-0.

[5] A. Albukhari, F. Lima, and U. Mescheder, "Bed-Embedded Heart and Respiration Rates Detection by Longitudinal Ballistocardiography and Pattern Recognition," *Sensors 2019, Vol. 19, Page 1451*, vol. 19, no. 6, p. 1451, Mar. 2019, doi: 10.3390/S19061451.

[6] R. González-Landaeta, O. Casas, and R. Pallàs-Areny, "Heart rate detection from an electronic weighing scale," *Physiol Meas*, vol. 29, no. 8, pp. 979–988, Aug. 2008, doi: 10.1088/0967-3334/29/8/009.

[7] Inan OT, Migeotte PF, Park KS, Etemadi M, Tavakolian K, Casanella R, Zanetti J, Tank J, Funtova I, Prisk GK, Di Rienzo M., "Ballistocardiography and seismocardiography: a review of recent advances," *IEEE J Biomed Health Inform*, vol. 19, no. 4, pp. 1414–1427, Jul. 2015, doi: 10.1109/JBHI.2014.2361732.

[8] I. Starr, A. J. Rawson, H. A. Schroeder, and N. R. Joseph, "Studies on the estimation of cardiac ouptut in man, and of abnormalities in cardiac function, from the heart's recoil and the blood's impacts; the ballistocardiogram" *https://doi.org/10.1152/ajplegacy.1939.127.1.1*, vol. 127, no. 1, pp. 1–28, Jul. 1939, doi: 10.1152/AJPLEGACY.1939.127.1.1.

[9] P. S. Luna-Lozano and C. Alvarado-Serrano, "Time and amplitude relationships of the ballistocardiogram in vertical and horizontal direction," *CCE 2012 - 2012 9th International Conference on Electrical Engineering, Computing Science and Automatic Control*, 2012, doi: 10.1109/ICEEE.2012.6421181.

[10] J. Gomez-Clapers, R. Casanella, and R. Pallas-Areny, "A Novel Algorithm for Fast Ballistocardiogram Cycle Extraction in Ambulatory Scenarios,"*2016 computing in Cardiology Conference (CinC),* 2016, doi: 10.22489/CINC.2016.102-371

[11] Y. Huang, C. Sun, T. Jin, S. Yang, and Z. Zhang, "Unobtrusive Inter-beat Interval Estimation from Multichannel Ballistocardiogram Signal Using Kalman Filter," *Proceedings of the Annual International Conference of the IEEE Engineering in Medicine and Biology Society, EMBS*, vol. 2020-July, pp. 455–460, Jul. 2020, doi: 10.1109/EMBC44109.2020.9176247.

[12] C. Alvarado-Serrano, P. S. Luna-Lozano, and R. Pallàs-Areny, "An algorithm for beat-to-beat heart rate detection from the BCG based on the continuous spline wavelet transform," *Biomedical Signal Processing and Control*, vol. 27, pp. 96–102, May 2016, doi: 10.1016/J.BSPC.2016.02.002.

[13] S. Gilaberte, J. Gómez-Clapers, R. Casanella, and R. Pallas-Areny, "Heart and respiratory rate detection on a bathroom scale based on the ballistocardiogram and the continuous wavelet transform," *Annu Int Conf IEEE Eng Med Biol Soc*, vol. 2010, pp. 2557–2560, 2010, doi: 10.1109/IEMBS.2010.5626866.

[14] O. A. Postolache, P. M. B. S. Girao, J. Mendes, E. C. Pinheiro, and G. Postolache, "Physiological parameters measurement based on wheelchair embedded sensors and advanced signal processing," *IEEE Transactions on Instrumentation and Measurement*, vol. 59, no. 10, pp. 2564–2574, Oct. 2010, doi: 10.1109/TIM.2010.2057590.

[15] I. Sadek, J. Biswas, B. Abdulrazak, Z. Haihong, and M. Mokhtari, "Continuous and Unconstrained Vital Signs Monitoring with Ballistocardiogram Sensors in Headrest Position," *2017 IEEE EMBS International Conference on Biomedical and Health Informatics, BHI 2017*, pp. 289–292, Feb. 2017, doi: 10.1109/BHI.2017.7897262.

[16] J. Paalasmaa, H. Toivonen, and M. Partinen, "Adaptive heartbeat modeling for beat-to-beat heart rate measurement in ballistocardiograms," *IEEE Journal of Biomedical and Health Informatics*, vol. 19, no. 6, pp. 1945–1952, Nov. 2015, doi: 10.1109/JBHI.2014.2314144.

[17] I. Sadek and B. Abdulrazak, "A comparison of three heart rate detection algorithms over ballistocardiogram signals," *Biomedical Signal Processing and Control*, vol. 70, p. 103017, Sep. 2021, doi: 10.1016/J.BSPC.2021.103017.

[18] I. Sadek and J. Biswas, "Nonintrusive heart rate measurement using ballistocardiogram signals: a comparative study," *Signal, Image and Video Processing*, vol. 13, no. 3, pp. 475–482, Apr. 2019, doi: 10.1007/S11760-018-1372-Z.

[19] A. Suliman, C. Carlson, C. J. Ade, S. Warren, and D. E. Thompson, "Performance Comparison for Ballistocardiogram Peak Detection Methods," *IEEE Access*, vol. 7, pp. 53945–53955, 2019, doi: 10.1109/ACCESS.2019.2912650.

[20] C. Carlson, V. R. Turpin, A. Suliman, C. Ade, S. Warren, and D. E. Thompson, "Bed-Based Ballistocardiography: Dataset and Ability to Track Cardiovascular Parameters," *Sensors (Basel)*, vol. 21, no. 1, pp. 1–13, Jan. 2021, doi: 10.3390/S21010156.

[21] S. G. Mallat, "A Theory for Multiresolution Signal Decomposition: The Wavelet Representation," *IEEE Transactions on Pattern Analysis and Machine Intelligence*, vol. 11, no. 7, pp. 674–693, 1989, doi: 10.1109/34.192463.

[22] M. Unser, A. Aldroubi, and S. J. Schiff, "Fast Implementation of the Continuous Wavelet Transform with Integer Scales," *IEEE Transactions on Signal Processing*, vol. 42, no. 12, pp. 3519–3523, 1994, doi: 10.1109/78.340787.

[23] J. Martin Bland and D. G. Altman, "Statistical methods for assessing agreement between two methods of clinical measurement," *The Lancet*, vol. 327, no. 8476, pp. 307–310, Feb. 1986, doi: 10.1016/S0140-6736(86)90837-8.

[24] C. Alvarado, J. Arregui, J. Ramos, and R. Pallàs-Areny, "Automatic detection of ECG ventricular activity waves using continuous spline wavelet transform," in *2nd International Conference on Electrical and Electronics Engineering, ICEEE and XI Conference on Electrical Engineering, CIE 2005*, 2005, vol. 2005, pp. 189–192. doi: 10.1109/ICEEE.2005.1529605.

[25] ANSI/AAMI EC13:2002, "Cardiac monitors, heart rate meters, and alarms", ANSI Standard, 2002.